Experimental studies on silicate structures of basaltic glasses quenched at 1 650℃ and 1—3.5 GPa

ZHU Weiguo[1], XIE Hongsen[1], XU Jian[2], HOU Wei[1], ZHANG Yueming[1], GUO Jie[1] and XU Zhuming[1]

1. *Earth's Interior Material Laboratory, Institute of Geochemistry, Chinese Academy of Sciences, Guiyang* 550002, *China*;
2. *Institute of Earth Science, Academia Sinica, Taibei, Taiwan, China*

Abstract A series of melting experiments was carried out at 1 650℃ and 1.00—3.00 GPa using alkaline basalt as starting material. The compositions of quenched basaltic glasses in the products were detected by electron micro probe. Their CIPW norms were calculated and their refractive indices were determined by the oil-infused method. The Raman spectrum of the quenched basaltic glasses indicates that their main structural species are monomer $[SiO_4]^{4-}$, chain $[Si_2O_6]^{4-}$ and sheet $[Si_2O_5]^{2-}$. The relationship at the same temperature between the proportions of integrated areas of structural species, and compositions and pressures was discussed.

Keywords: quenched basaltic glass, structure of melt, Raman spectrum.

MELTING is one of the important mechanisms of earth's materials evolution. The transport and crystal-

lization of silicate melts and the interactions between melts and rocks can cause the movement and differentiation of earth's interior materials, and even make local material homogenization under the given conditions. It is of essential significance to investigate the structures of silicate melts. It has been proved that the structures of quenched silicate glasses are principally similar to those of silicate melts at high temperature, and it is an effective way to study the structures of melts and to discuss the relationship between the structures of the melts and their composition, temperature, and pressure by using quenched glasses. In recent years, *in-situ* measurements of the structures of the melts at 1 atm. and high temperature show that there is no great difference between the structures of quenched glasses and those of the melts[1, 2]. But it is hardly possible to carry out the *in-situ* measurements of the structures of silicate melts at high temperature and high pressure due to the restriction of the apparatus generating high pressure, thus the way to use quenched glasses to study the structures of melts is still commonly available. Basalt is most widely distributed on the earth's surface and its genesis is related with plate destruction and mantle magmation. In this study, we measured the compositions and structures of the quenched basaltic glasses, using the alkali basalt from Southeast China as starting material, to provide the experimental basis for discussing its properties and structures.

1 Starting material and method

The starting material used in our experiments was alkali basalt from Qianyang, Minqing, Fujian Province, which contains a lot of spinel lherzolite xenolithic enclaves and clinopyroxene megacrysts. The basalt which bears no enclaves and megacrysts was ground as fine as 200 mesh and dried at 80—100℃ for about 2 h before experiment. Its chemical composition is given as: SiO_2 48.86, TiO_2 2.12, Al_2O_3 13.25, Fe_2O_3 2.16, FeO 7.84, MnO 0.11, MgO 9.03, CaO 9.64, Na_2O 3.15, K_2O 1.56, H_2O^+ 1.25, H_2O^- 0.83, P_2O_5 0.62 (%). The NBO/T of such melt deduced from its chemical composition was 1.015 (NBO/T represents the number of non-bridging oxygen to tetrahedrally coordinated cation in the melt, which is an index to indicate the degree of coordinating in the melt; T usually represents cations such as Si^{4+}, Al^{3+}).

The sample assembly is shown in fig. 1. The pyrophillite cube (32 mm × 32 mm × 32 mm) as the pressure-transfer medium was baked at 650℃, and the pyrophillite stem and insulating pyrophillite tube were baked at 800℃ to avoid the influence of water in the experimental system. The sample cell was made of graphite which is stable under experimental temperature and pressure with no influence on the composition. The sample cell was 8 mm in length and 6 mm in diameter and was placed at the middle part of the heating system to minify the gradient of temperature. Experimental study on this basalt carried out by Ren showed that its melting points were in the range 1 400℃ (1 GPa)—1 500℃ (3.5 GPa)[3]. In our experiments, the temperature was 1 650℃ at varying pressures and was calibrated by $PtRh_{10}$-Pt thermocouple to be sure that the specimen was above the liquid phase temperature.

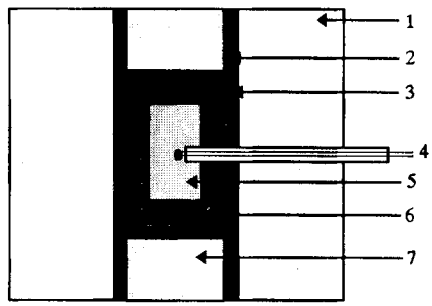

Fig. 1. Sample assembly. 1, Pyrophillite; 2, steel ring (ø14—12 mm); 3, graphite tube (ø14—12 mm); 4, thermocouple ($PtRh_{10}$-Pt); 5, sample cell (ø8—6 mm); 6, insulating pyrophillite (ø12—8 mm); 7, pyrophillite stem.

Our experiments were carried out in the cubic anvil apparatus on the YJ-3000T pressure machine at the Institute of Geochemistry, the Chinese Academy of Sciences. In our experiments, first the pressure was raised to the scheduled pressure and the temperature was raised to 1 650℃ step by step, keeping the highest temperature for half an hour, followed by quenching. The quenching rate was greater than 180℃/s at the first 3 s. Detailed description about the calibrations of temperature and pressure has been reported[4].

2 Experimental results

The experimental products were snuffcolored cylindrically geometric glasses. Microscopic examination of the polished section prepared from the transverse section of the product revealed that the product was composed mainly of melt phase and few nucleations. The nucleations formed a circle at the edge of the

transverse section, whose amount increased with pressure and even appeared at the center of the section above 2.0 GPa. Electron microprobe analysis showed that the composition of the nucleation was augite. Table 1 shows the experimental conditions, the results of electron microprobe analysis of the melt phases (quenched basaltic glasses), the refractive indices and the results of the CIPW normative mineral calculation. The total amounts of oxides analyzed by JCXA-733 Electron Probe were 93.02—101.04. The solubility of water in the melts might cause the deficiency of the total amounts.

Table 1 Results of electron microprobe analysis of basaltic glasses, CIPW and experimental conditions

Sample No.	1	2	3	4	5
Pressure/GPa	1.00	1.50	2.00	2.50	3.00
Refractive index	1.592 9	1.597 8	1.603 8	1.609 9	1.611 3
		weight percentage of oxide			
SiO_2	52.25	49.15	49.02	47.86	47.59
Al_2O_3	13.15	13.40	13.17	14.34	14.24
FeO	10.25	9.33	8.41	9.71	7.38
MgO	9.48	9.00	9.09	8.55	9.03
CaO	8.71	8.57	8.45	8.32	7.62
MnO	0.00	0.21	0.00	0.09	0.00
Na_2O	2.91	2.48	2.69	2.56	2.93
K_2O	1.65	1.44	1.49	1.34	1.55
Cr_2O_3	0.01	0.25	0.08	0.18	0.31
TiO_2	1.73	1.78	1.82	1.57	1.58
P_2O_5	0.90	0.63	0.68	0.85	0.79
Total	101.05	96.23	94.88	95.38	93.02
Al/(Al + Si)	0.23	0.24	0.24	0.26	0.26
		results of CIPW normative mineral calculation			
Or	9.65	8.85	9.30	8.31	9.87
Ab	24.38	21.90	23.97	22.75	26.71
An	17.75	22.04	20.52	24.88	22.81
Di	15.63	14.66	15.39	10.34	9.98
Hy	15.63	17.00	14.79	14.92	10.05
Ol	11.54	10.42	10.62	13.50	15.26
Il	3.24	3.52	3.65	3.14	3.24
Ap	1.95	1.43	1.57	1.95	1.87

Table 1 shows that the compositions of the glasses quenched at different pressures and the same temperature are quite similar, but there are still some differences with pressure increasing and nucleating. Al_2O_3 and SiO_2, which greatly affect the structures of the melts, have an increasing trend and are higher than those of the starting material when the pressure is increased. Al/(Al + Si) shows the same trend (fig. 2 and table 1). The results of the CIPW normative mineral calculation show that the quenched basaltic glasses belong to the system (Or, Ab, An)-(Di, Hy)-Ol.

Table 1 also shows that the refractive index of the glasses tends to increase with pressure increasing, which indicates that the densities of the glasses are increasing with pressure increasing because their refractive index responses to their density. The results of electron microprobe analysis of the glasses quenched at different pressures show that there is some difference except that Al_2O_3 shows a trend of an increase. Therefore, it is inferred that the increasing of refractive index and densities of basaltic glasses may be explained by the following two reasons: (1) the changes in struc-

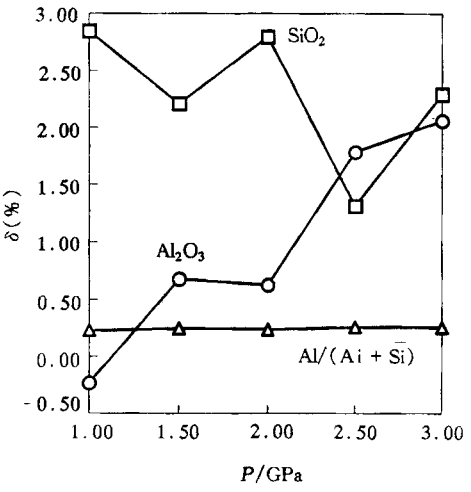

Fig. 2. Relationship between SiO_2, Al_2O_3 and pressures at 1 650℃. δ, Difference of oxides (SiO_2, Al_2O_3) in quenched glasses and starting material.

ture of the basaltic glasses induced by the compositions; and (ii) the changes in structure induced by pressure. We examined thestructures of the basaltic glasses by Raman Spectroscopy to prove the supposition. The Raman Spectroscopy used here is of Renishaw 2100 model, which has a resolution down to 0.1 cm^{-1}. The samples were excited with 514.5 nm-line Ar^{+} laser operating at 800 mW. Fig. 3 shows a typical Raman spectrum of the basaltic glasses. Table 2 shows the results obtained from Gaussian statistical curve-fitting of Raman spectra of the glasses.

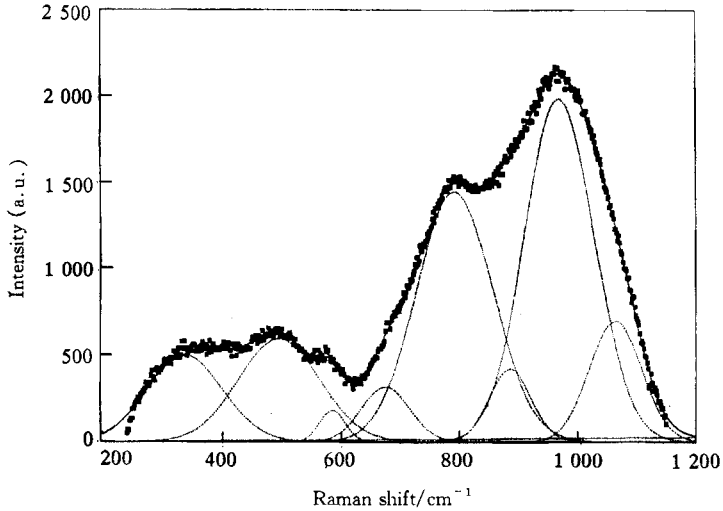

Fig. 3. Raman spectrum of the quenched basaltic glass.

Table 2 Results of Raman spectroscopic investigation of basaltic glasses

Sample No.		ν1	ν2	ν3	ν4	ν5	ν6	ν7	ν8
1	frequency	341.5	490.5	579.4	676.6	796.2	890.2	973.6	1 065.2
	S(%)	9.47	10.05	1.73	4.19	27.64	5.98	32.73	8.20
2	frequency	345.5	497.4	582.1	673.9	796.1	889.9	973.1	1 063.3
	S(%)	8.99	8.85	1.65	3.46	29.92	4.51	34.41	8.21
3	frequency	341.5	499.9	585.5	679.4	795.3	890.2	972.5	1 063.9
	S(%)	7.88	9.8	1.66	4.23	27.67	6.09	33.52	9.76
4	frequency	337.2	500.2	581.2	675.0	795.6	889.7	972.0	1 062.4
	S(%)	8.17	10.34	1.05	3.61	29.04	4.90	33.57	9.31
5	frequency	346.9	504.8	585.2	671.7	793.5	887.9	973.0	1 063.4
	S(%)	9.56	8.75	1.74	3.01	29.53	2.91	37.64	6.85

The experimental conditions are the same as in table 1. S presents the proportion of integrated area.

3 Discussion

As shown in table 2, the Raman spectra of the basaltic glasses are quite complicated. According to previous studies, band ν1 (337—347 cm^{-1}) is assigned to the vibration of M-O in the melt (M as alkali or alkaline-earth cation) and O-Si-O; band ν2 (490—504 cm^{-1}) to the deformation and rocking model of three-dimensional net-work structure; band ν3 (579—585 cm^{-1}) to the rocking model of bridging oxygen of species containing non-bridging oxygen; band ν4 (671—676 cm^{-1}) to the deformation of O-Si (Al)-O angle; band ν5 (793—796 cm^{-1}) to the bending vibration of O-Si(Al)-O; band ν6 (887—890 cm^{-1}) to the stretch vibration of Si-O_{nb} (O_{nb} represents non-bridging oxygen) in $[SiO_4]^{4-}$ species[5, 6]; band ν7 (~973 cm^{-1}) to the stretch vibration of Si-O_{nb} in the species containing 2 non-bridging oxygens[5, 7], for example, chain species $[Si_2O_6]^{4-}$; band ν8 (~1 063 cm^{-1}) to the stretch vibration of Si (Al)-O_{nb} in the species containing 1 non-bridging oxygen, such as sheet species $[Si_2O_5]^{2-}$. Although the starting material was dried before experiment, the very weak band near 3 500 cm^{-1} in the Raman spectra of basaltic glasses showed that a small amount of water was dissolved in the melts because the water in the analcite contained in the starting material could not be driven out.

Therefore, the Raman spectra indicate that there are three structural species in the basaltic glasses: $[SiO_4]^{4-}$ (monomer), $[Si_2O_6]^{4-}$ (chain) and $[Si_2O_5]^{2-}$ (sheet). This is in agreement with the conclusion of Virgo *et al.*[8], who found that $[SiO_4]^{4-}$ (monomer), $[Si_2O_6]^{4-}$ (chain) and $[Si_2O_5]^{2-}$ (sheet) structural species occurred in the system for NBO/T 2—1.

Table 2 shows that the frequencies of the structural species in the basaltic glasses do not shift distinctly, but their proportions of integrated areas change properly with pressure increasing (fig. 4). The proportion of $[Si_2O_6]^{4-}$ (chain) tends to increase with pressure increasing, but that of $[SiO_4]^{4-}$ (monomer) and $[Si_2O_5]^{2-}$ (sheet) shows an opposite trend. This phenomenon is more obvious at pressure of higher than 2.00 GPa, which indicates that there is a reaction in the melts as follows:

$$[SiO_4]^{4-}\text{ (monomer)} + [Si_2O_5]^{2-}\text{ (sheet)} \Rightarrow [Si_2O_6]^{4-}\text{ (chain)}$$

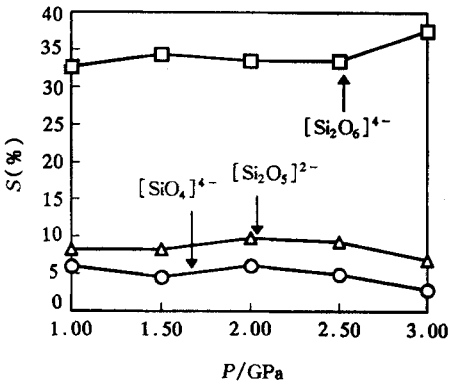

Fig. 4. Relationship between proportions (S) of integrated areas of structural species and pressures (P).

Combined with the change in composition of the basaltic glasses with pressure, Al_2O_3 trends to increase with pressure increasing, it is suggested that Al^{3+} in the melts usually substitutes the Si^{4+} of fully polymerized anionic constitution such as $[SiO_2]^0$, but with pressure increasing, Al^{3+} may gradually enter the $[Si_2O_5]^{2-}$ (sheet) and $[Si_2O_6]^{4-}$ (chain) species. It means that the rise of pressure will be favorable to shifting the reaction to the right and makes the melts depolymerized. Therefore, the viscosities of the melts will decrease consequently. The conclusion about the viscosity can be proved by the changes in the amounts of nucleations in basaltic glasses. According to the theories of homogeneous nucleation or inhomogeneous nucleation[9, 10], nucleation rate I in the melt is inverse to its viscosity η, viz. $I \propto 1/\eta$. The phenomenon observed under a microscope showed that the nucleations appeared in the center of the sample when pressure was higher than 200 GPa. Furthermore, the amounts of nucleation increased with pressure increasing, i.e. the nucleation rate increased. This showed, on the other hand, that viscosity decreased with pressure increasing. According to the effect of subtrate in the theory of inhomogeneous nucleation, the first crystallized phase is the main part of structural species in the melt. In our experiments, the electron microprobe analysis showed that what was involved in the nucleation is augite with chain structures. This has also proved that the proportions of chain species ($[Si_2O_6]^{4-}$) increased with pressure increasing and the reaction shifted to the right.

In conclusion, this experimental investigation shows that the structural change of basaltic melts at high pressure are affected by the following factors: (ⅰ) structural changes induced by chemical compositions of the melt; (ⅱ) changes in equilibrium induced by pressure in the structural species existing in the melt. They are interdependent because the chemical compositions of the basaltic melts were affected by pressure to a certain extent.

Acknowledgement This work was supported by the National Natural Science Foundation of China (Grant No. 49772111).

References

1 Naniel, R. N. Mysen, B. O., Role of aluminium in the silicate network: *In situ*, high-temperature study of glasses and melts on the join SiO_2-$NaAlO_2$, *Geochimica et Cosmochimica Acta*, 1996, 60(10): 1727.
2 Bjorn, M., Haploadndesitic melts at magmatic temperatures: *In situ*, high-temperature structure and properties of melts along the join $K_2Si_4O_9$-$K_2(Kal)_4O_9$ to 1 236℃ at atmospheric pressure, *Geochimica et Cosmochimica Acta*, 1996, 60(19): 3665.
3 Ren Guohao, Xie Hongsen, Xie Xiande, An experimental study on the melting-crystallization of basalt at high pressures, *Geochemica* (in Chinese), 1990(3): 249.
4 Xie Hongsen, *Introduction of Materials Science of Earth's Interior* (in Chinese), Beijing: Science Press, 1997, 44—47.
5 Mysen, B. O., Virgo, D., Seifert, F., Melt structures and redox equilibria in the system CaO-MgO-FeO-Fe_2O_3-SiO_2, *Annual Report of the Director Geophysical Laboratory, Carnegie Institution* 1978—1979, 1979, 519—526.
6 Furukawa, T., Brawer, S., White, W. B., the structure of lead silicate glasses determined by vibrational spectroscopy, *J.*

Mater. Sci., 1978(13): 268.
7 Brawer, S. A., White, W. B., Raman spectroscopic investigation of structure of silicate glasses: Ⅱ Soda-alkali earth-alkali ternary and quaternary glasses, *J. Non-cryst. Solid*, 1977, 23: 261.
8 Virgo, D., Mysen, B. O., Kushiro, I., Anionic constitution of 1-atm silicate melts: implications for the structure of igneous melts, *Annual Report of the Director Geophysical Laboratory*, *Carnegie Institution* 1979—1980, 1980, 310—311.
9 Kirkpatrik, R.J., Theory of nucleation in silicate melts, *Am. Mineral.*, 1983, 68: 66.
10 Cashman, K.V., Textural constrains on the kinetics of crystallization of igneous rocks, *Modern Methods of Igneous Petrology: Understanding Magmatic Processes*, *Reviews in Mineralogy*, 1990, 24: 259.

(*Received April* 27, 1998)